

M. Bergamasco
F. Salsedo
M. Fontana
F. Tarri
C.A. Avizzano
A. Frisoli
E. Ruffaldi
S. Marcheschi

High performance haptic device for force rendering in textile exploration*

Published online: 2 March 2007
© Springer-Verlag 2007

Abstract The HAPTEX system aims to develop a new multi-sensory environment for the immersive exploration of textiles.

HAPTEX is based on a multi-layer/multi-thread architecture that optimizes the computational speed and integrates three different types of sensory feedback: vision, tactile and haptic.

Such kind of environment is suitable for demanding VR applications such as the online marketing of novel textiles or garments, however it requires the design of a high performance multi-point haptic interface.

The present work focuses on the haptic device design and describes how demanding requirements can

be met by integrating on a high performance device a force sensor to achieve closed loop control.

The methodology for the dimensioning of a motion based explicit force control on the basis of the dynamic parameters will be discussed and the specific implementation for the HAPTEX system presented.

Keywords Haptic interfaces · Textile modeling · Visual/tactile integration

M. Bergamasco (✉) · F. Salsedo ·
M. Fontana · F. Tarri · C.A. Avizzano ·
A. Frisoli · E. Ruffaldi · S. Marcheschi
PERCRO, Scuola Superiore Sant'Anna,
Pontedera, Italy
m.bergamasco@sssup.it

1 Introduction

The ability to assess, in virtual environments, cloth or garments, as they are actually touched by the user, is of central importance in the selection-for-purchase process of every consumer [12].

The realistic rendering of the physical interaction of the hand with fabrics implies the accurate generation of very small global and spatially distributed forces, of the order of few grams.

Related major challenges require the design of new algorithms for the real-time representation of visual and contact stimuli and the design of new devices for the sim-

ultaneous representation of force and tactile information during exploration and manipulation [14].

A large amount of research has been carried out to develop physically based models that are suitable for real-time simulation [4, 5] of fabrics. As far as the physical models are concerned, the most used ones are particle models [11] and finite element models [8].

In recent years, haptic interfaces have received increasing attention from researchers for their potential applications in industry and society, and also of their versatility that make them suitable to different applications.

Govindaraj envisaged [9] the possibility to enrich the virtual interaction with digital clothes by integrating haptics and tactile displays. He made use of a tactile pin array attached to the end-effector of a planar haptic interface for the rendering of the fine mechanical properties of virtual fabrics. However the kinematic constraints of his solution

*The present work has been supported by the EU within the context of the following projects: HAPTEX, ENACTIVE

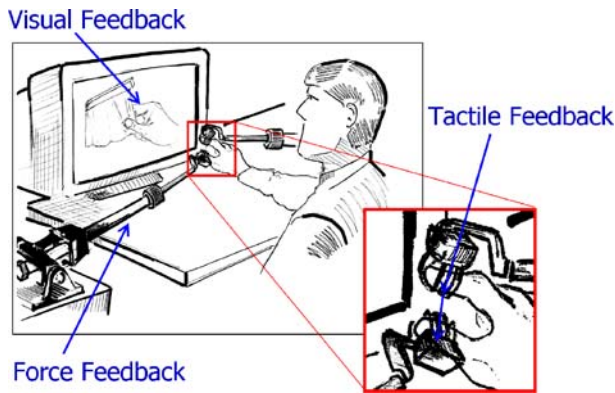


Fig. 1. HAPTEX scenario

limit the exploration to rigid planar garments with planar force rendering.

When a spatial interaction is required, more complex models and control algorithms for the HI are needed, as outlined in the survey by Buss et al. [15]. Several works on the control of HI with explicit force control have been carried out in [1, 16, 17], but none of them have investigated the control of mechanical structures with very high compliance. A possible schematization and analysis of explicit force controllers that takes into account the compliance of the mechanical system is done by Eppinger in [6] within the field of control of manipulators.

However, when a haptic interface is employed as force display device in textiles exploration and manipulation, the application context poses strict requirements on the device performances that may be difficultly achieved with existing systems: from one side manipulation of textiles requires multiple points of contact, each one exerting forces up to several Newtons, on the other side fine surface exploration of textiles requires of the same device a force resolution and accuracy of few grams.

Presently, all commercially available HIs do not comply with these demanding requirements. This has been the main motivation for the development of a new device, a force sensor and the related closed loop controller. The device is based on the existing GRAB system [3], that already solved the issues of multi-point cooperative haptic interaction in large workspaces.

In this paper we introduce the overall system architecture that has been conceived to integrate the sensorial feedback and discuss the technical features of the novel HI. Moreover an optimal design procedure for the closed loop control is presented. Such a procedure is based on an inverse model of the human impedance, which has been estimated as a relevant component of the control design. The identification of the user is based on the specific configuration of the device (finger hold in a thimble) and extending previous works on other given configurations: finger on a plate [10], against a wall [18], during precision grasping [7].

2 Architecture of the HAPTEX system

The HAPTEX system integrates three different displays: a haptic interface, a visualization system and a tactile display (Fig. 1).

All of them share a common VR scenario representing a virtual textile, modeled through a square cloth.

The cloth is fixed on a horizontal stand such that, in resting condition the steady state solution is determined solely by the gravity force.

The physical interaction can be attained through the index finger and the thumb. The user can touch, squeeze, rub and stretch the fabric, feeling the corresponding global forces on the fingertips arising from the deformation of the textile and the tactile stimulation due to the relative motion of the finger with respect to the deformed surface.

During the virtual simulation such forces will be displayed by the haptic device and a tactile display attached to user fingertips.

The system should be able to reproduce a physical effect at such levels of detail such that: physical interaction with the fingertips may occur in every part of the cloth; the two fingertips may independently act on the same piece of textile; friction and slip effect between fingertips and textile may occur according to physical condition.

The complexity of the simulation suggested to adopt a two-layer architecture, using different models for each layer as proposed in [2]: one Large Scale Model (LSM) that evaluates the cloth dynamics in the region far from the contact points, and a Small Scale Model (SSM) that models the contact properties in regions close to the fingertips.

The two models operate at different frequencies (25 Hz for LSM, 1000 Hz for SSM) according to the requirements of different display devices. An impedance network matches constraints between models at boundary regions as shown in Fig. 2.

Clothes models have been derived for a broad range of fabrics (32 different samples). The measurements were performed using the KES-F system [13], which is the most

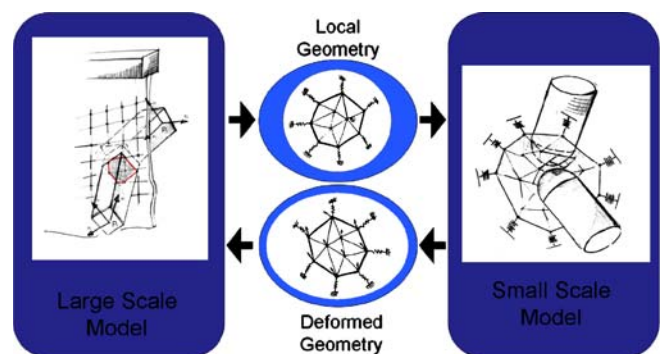


Fig. 2. Interconnection between LSM and SSM

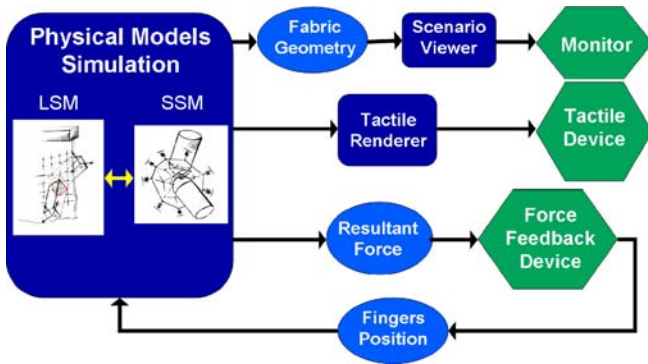


Fig. 3. Scheme of the architecture of the HAPTEX system

common method for objective evaluation of fabric. According to this method the fabric is modeled by parameters representing the measurements of bending, tensile, shearing, compression, friction and roughness.

The overall architecture is described in Fig. 3: the Physical Model Simulation (PMS) delivers the rendering information to all the system display devices.

3 Design of the HI

The design of the novel HI took as reference the work developed for the GRAB system [3]. GRAB is a 6-DOF desktop force-feedback device with a serial kinematics. The device is composed of two identical units each of them providing forces at the level of one of the user's fingertips as shown in Fig. 4.

In the modified design of the device, the first 3 DOFs (RRP) are required to track the position of the fingertip in 3D space and the remaining 3 (RRR) are required to track its orientation. All DOFs are provided with high resolution angular sensors. Moreover, motors on the first 3 DOFs may exert on the user's fingertip forces of arbitrary orientation and modulus, whereas the last 3 DoFs are passive. The three motors are remotely located in order to reduce

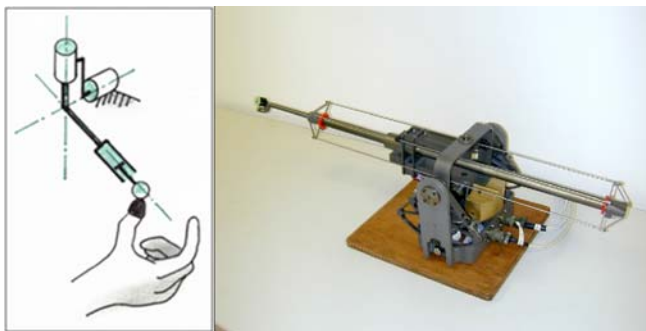


Fig. 4. Kinematics and photo of one arm of the GRAB

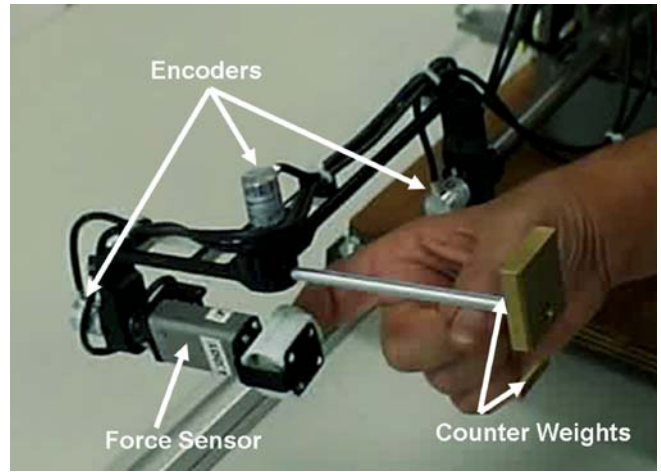


Fig. 5. A detail of the force sensor in the GRAB modified version

the overall weight and inertial effects: the first two actuators are mounted on the fixed link (base), while the third actuator is mounted in the equilibrium center of the second moving link. Forces are transmitted from the actuators to the joints by steel cables routed on idle pulleys. This modified version was equipped with a new high resolution three-axial force sensor, purposely designed to read forces exerted by the fingertip on the HI contact point, as shown in Fig. 5.

4 Control design

The control loop has been implemented on a 850 MHz Pentium III, equipped with an ISA I/O board (ServoToGo Model II – 8 axis); additional 16 bit ADC electronics has been implemented for converting force sensor data. Motor power is supplied by 6 PWM drivers (Elmo Violin 10/100).

Figure 6 shows the general scheme of the control architecture for each DoF that has been selected for the

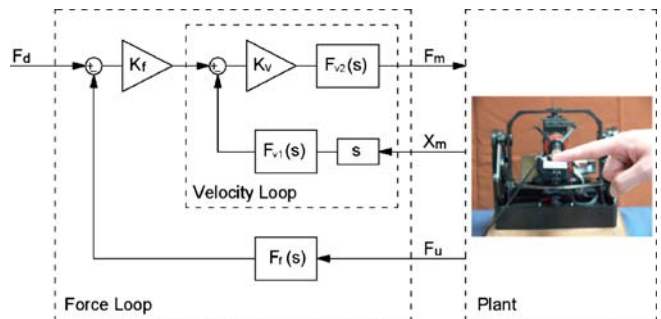


Fig. 6. General control scheme

implementation of the explicit force control: it consists of an inner velocity loop-outer force loop scheme. This one-dimensional scheme can be simply generalized for implementing a three-dimensional force control: it is sufficient to transform the velocity reference, obtained as output of gain K_f , in a joint speed reference by simply multiplying it with the inverse of the Jacobian matrix, which describes the inverse differential kinematics of the device.

This solution allows general control architecture to be safe and simplifies the interface procedure with user.

4.1 Physical model of the mechanics

The mechanical architecture used for the haptic interface allows the following schematization for the dynamics of each DOF: two masses representing the inertia of motor and link; a spring, connecting the motor and the link reduced masses, representing the transmission stiffness; two dampers, connecting the motor and the link masses to the ground, representing the viscous friction located in moving parts (mainly bearings); a mass-spring-damper system, connected rigidly to the link, representing the human finger dynamic. A schematic representation of the joint dynamic model is shown in Fig. 7.

All the model parameters and variables introduced below are expressed with respect to the same axis. Moreover, the linear moving elements indicated in the scheme of Fig. 7 could schematize also rotating parts. The transfer function between the motor force F_m and the motor position X_m is:

$$\frac{X_m}{F_m} = \frac{1}{K_u} \times \frac{\frac{s^2}{s_g^2} + \frac{s_{cg}s}{s_g^2} + 1}{\frac{s^4}{s_r^2 s_u^2} + \left(\frac{s_{cm} + s_{cg}}{s_u}\right) \frac{s^3}{s_r^2 s_u} + \left(\frac{s_r^2 + s_{cm} s_{cg}}{s_r^2}\right) \frac{s^2}{s_u^2} + \frac{s_{ctot}s}{s_u^2} + 1} \quad (1)$$

where

$$s_u = \sqrt{\frac{K_u}{M_{tot}}}; \quad s_r = \sqrt{\frac{K_t}{M_r}}; \quad s_g = \sqrt{\frac{K_t}{M_g + M_u}};$$

$$s_{cm} = \frac{C_m}{M_m}; \quad s_{cg} = \frac{C_g + C_u}{M_g + M_u}; \quad s_{ctot} = \frac{C_m + C_g + C_u}{M_{tot}};$$

$$M_{tot} = M_m + M_g + M_u; \quad M_r = \frac{M_m(M_g + M_u)}{M_{tot}}.$$

The frequency s_g is called anti-resonant frequency of a two-mass system while s_r is the resonant frequency.

The following assumptions can be applied to this kind of haptic interface:

1. The motor mass is much lower than the joint mass, so $s_g \ll s_r$.
2. The motor and the joint damping factors are much lower than 1, so $s_{cg} \ll s_g$ and $s_{cm} \ll s_r$.

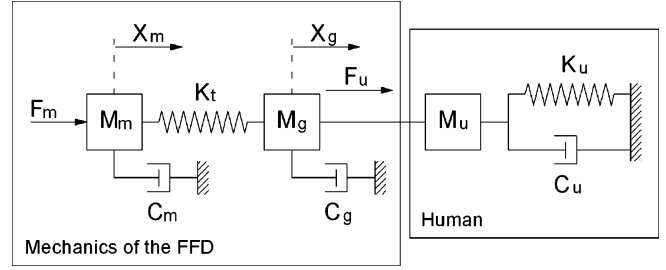


Fig. 7. One DOF mechanical model

These assumptions allow to simplify Eq. 1 in:

$$\frac{X_m}{F_m} = \frac{1}{K_u} \frac{\frac{s^2}{s_g^2} + \frac{s_{cg}}{s_g} \frac{s}{s_g} + 1}{\frac{s^2}{s_r^2} \frac{s^2}{s_u^2} + \left(\frac{s_{cm} + s_{cg}}{s_u}\right) \frac{s^2}{s_r^2} \frac{s}{s_u} + \frac{s^2}{s_u^2} + \frac{s_{ctot}}{s_u} \frac{s}{s_u} + 1}$$

Furthermore it is generally true that $K_u \ll K_t$. Consequently the transfer function between the force transmitted to the human finger F_u and the motor position X_m reduces to:

$$\frac{F_u}{X_m} = K_u \frac{\frac{s^2}{s_u'^2} + \frac{s_{cu'}}{s_u'} \frac{s}{s_u'} + 1}{\frac{s^2}{s_g^2} + \frac{s_{cg}}{s_g} \frac{s}{s_g} + 1} \quad (2)$$

where

$$s_u' = \sqrt{\frac{K_u}{M_u}}; \quad s_{cu'} = \frac{C_u}{M_u}$$

In Fig. 8 the asymptotic magnitude Bode plots of Eqs. 1 and 2 are reported.

The frequency of the zero of the human dynamics has been estimated to be lower than the frequency of the transmission pole. The red arrows shown in Fig. 8 indicate that a gain peak due to the resonance effect is expected in the real Bode plot.

Experimental validation. The dynamic response of the haptic interface has been investigated exciting each DOF of the HI separately. For each DOF, two separate sets of experiments have been carried out in order to validate and identify the theoretical transfer functions described above, using non-parametric methods, such as spectral analysis. For both sets of experiments a pseudo-random binary signal has been selected as an excitation signal for the actuator.

The first set of experiments was devoted to the validation of the transfer function in Eq. 1. During this experiment it was observed that the location of the poles and the zero of the transfer function is not significantly affected by the presence of the user impedance applied at the end-effector. This is attributable to the negligible value of the stiffness of the mass of the human finger when compared to the corresponding parameters of the HI.

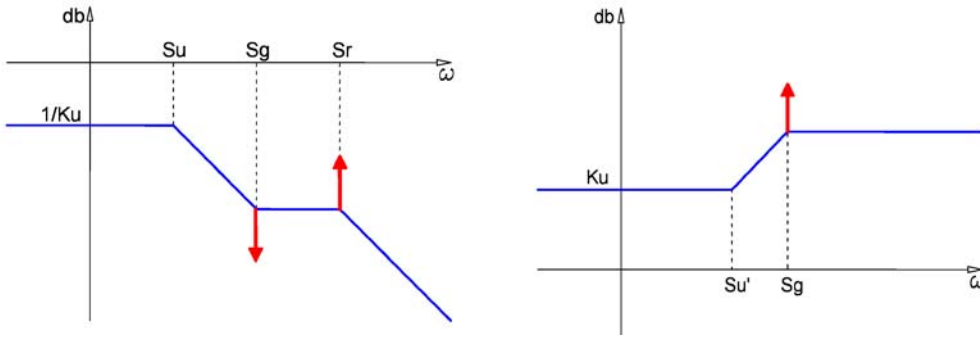


Fig. 8. One DOF theoretical Bode plot

The second set of experiments was devoted to the validation of the transfer function in Eq. 2. Since in this case the impedance of the user plays a major role in the pole-zero location, five different users were involved. The users were required to apply their own right-hand index finger in the gimbal of the HI, as shown in Fig. 5. The empirical transfer function estimation is computed as the ratio of the output Fourier transform to the input Fourier transform, using the Fast Fourier Transform (FFT) algorithm. Moreover, a smoothed version of the transfer function estimate algorithm has been used, obtained by applying a Hamming windowing transformation to the FFT of the output signal and to the absolute square of the FFT of the input.

Figure 9 shows the Bode plot of X_m/F_m experimental transfer function. A good agreement between the predicted asymptotic plot and the experimental one can be observed. The high resonant peak of double transmission poles s_r and zeros s_g confirm the assumption of low damping factor. The absence of resonances for the pole s_u indicates a human damping factor close to one.

In Fig. 10 the experimental Bode plots of the transfer function Eq. 2 relating to three of the five different

users is shown together with the theoretical asymptotic plot. The behavior represented in the figure can be interpreted as follows: the general trend is in accordance with the model only for frequencies over 10 Hz; for lower frequencies, the mass of the palm of the hand and the forearm contribute to the measured impedance and for this reason this cannot be represented by a simple second-order system; a sixth-order system should be necessary for representing the real dynamic response. The differences between the Bode plots demonstrate significant variability of the dynamic parameters (K_u, C_u, M_u).

The accuracy of the experimentally evaluated Bode plot increases with the level of the energy introduced in the system and with a proper selection of the maximum frequency content of the exciting signal. For both experiments a force signal switch from 0 to 8 N was used. The maximum frequency was set at 200 Hz.

Identification of the dynamic parameters. Only a subset of the model parameters has been estimated by experimental identification.

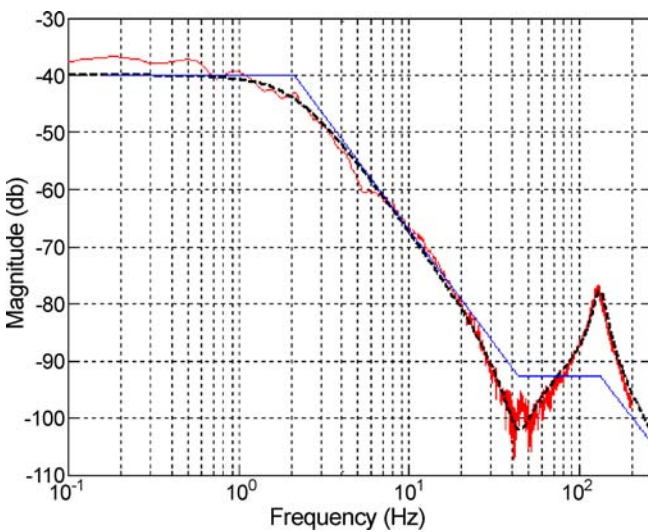


Fig. 9. Experimental X_m/F_m transfer function

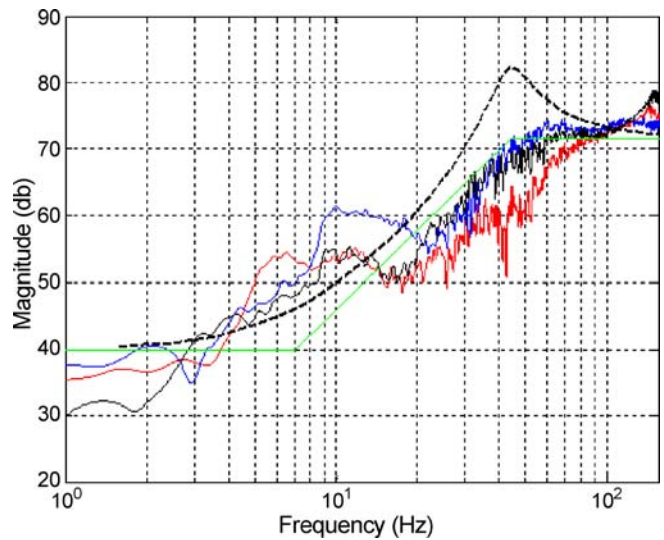


Fig. 10. Experimental F_u/X_m transfer function

The motor and the joint masses can be estimated with good accuracy by CAD models of the mechanical parts. Also, the transmission stiffness constant has been estimated using a theoretical model for the cable transmission (an elastic beam with a proper Young's modulus). The theoretical value has been validated with the experimental value, obtained by double zero transfer function where:

$$S_g \approx \sqrt{\frac{K_t}{M_g}}$$

Experimental identification has been performed for the viscosity coefficients and human model parameters. The device viscosity coefficients have been determined by fitting the model with the experimental Bode plot of Fig. 10.

Human model parameters have been estimated by using experimental Bode plots as follows:

Human stiffness could be estimated by considering the asymptotic value of Fig. 10 for $s \rightarrow 0$, in accordance with the theoretical transfer function Eq. 1, resulting in:

$$\left. \frac{X_m}{F_m} \right|_{s \rightarrow 0} = \frac{1}{K_u}$$

Observing the low frequency behavior of the Bode plots shown in Fig. 10, human damping factor can be assumed to be close to unity.

Human mass can be empirically estimated by correlating the Bode plot of Fig. 9 with the theoretical one. The measured parameters of the system are reported in Table 1. The reported stiffness value is the maximum observed among users while the obtained values of the finger mass remain almost constant for different persons.

5 Dimensioning procedure

For dimensioning the controller parameters of the general scheme shown in Fig. 6, first the inner velocity loop is di-

Table 1. Experimental values of model parameters

| Parameter | Value | Unit |
|-----------|---------------------|------|
| M_m | 0.062 | kg |
| M_g | 0.450 | kg |
| M_u | 0.050 | kg |
| K_t | 37.70×10^3 | N/m |
| K_u | 100 | N/m |
| C_m | 4.713 | Ns/m |
| C_g | 38.915 | Ns/m |
| C_u | 2.683 | Ns/m |
| s_u | 2.1 | Hz |
| s_g | 43.7 | Hz |
| s_r | 131.4 | Hz |

mentioned and then the parameters of the outer force loop are optimized.

5.1 Velocity loop

Observing the Bode plot of Fig. 9, two possible strategies can be followed: place the bandwidth of the velocity loop s_v below the double transmission zero s_g or over the double transmission pole s_r . The first solution has been adopted since the second one can be used only for systems equipped with velocity sensors like tachometers or alternatively with high resolution position sensors. Indeed in the case of limited resolution of the position sensors, the velocity feedback estimated by derivation from the position signal has to be filtered to relatively lower frequencies in order to avoid noises incompatible with the final application. In the case of the selected solution (bandwidth below s_g) the maximum theoretically reachable bandwidth is s_g . In order to achieve this maximum a filter F_{V1} has to be inserted in the forward path of the control loop for attenuating the resonant peak in correspondence of s_r . This filter should match the following requirements:

- (1) Keep the magnitude above 0 db for frequencies over the velocity bandwidth s_v ;
- (2) have a minimal phase lag at s_v (in order to guarantee a certain phase margin).

For selecting the best filter for this purpose, an analytical evaluation of different filters has been carried out: given the allowable phase lag ϕ_p and the desired attenuation at s_r , the different filters have been evaluated by considering the difference $s_r - s_p$, where s_p is the frequency at which the filter phase lag is equal to ϕ_p . Indeed the minimum value of the difference $s_r - s_p$ indicates that filter is able to produce the desired attenuation with minimal phase lag at lower frequency. A filter of a different type, order and cutoff frequency has been considered: the third-order Chebyshev Type I filter resulting as the best one.

The Chebyshev filter has been dimensioned in order to have an attenuation in s_r of 30 db and a phase lag of 60 degrees: on the basis of the specifications, the value for s_p was 27.8 Hz. The proportional gain K_v is then fixed in order to obtain the maximum bandwidth (open loop magnitude of 0 db for $s = s_p$) $K_v \approx \frac{M_{tot}}{s_p}$.

Finally, the filter F_{V2} is introduced for limiting the noise of the velocity signals derived from the encoder position. Its pole must be placed on a sufficiently high frequency for limiting its contribution to the phase lag.

Final velocity control parameters and performances are reported in Table 2.

Figure 11 shows the Bode diagram of open and closed loop velocity controller.

5.2 Force loop

For a frequency lower than its bandwidth the inner velocity controller has a transfer function close to the identity.

Table 2. Velocity control parameters

| Parameter | Sym. | Value | Unit |
|-----------------------|----------|-------|--------|
| Velocity gain | K_v | 98.4 | Ns/m |
| Fv1 cut-off frequency | f_{v1} | 500 | Hz |
| Fv2 cut-off frequency | f_{v2} | 59.6 | Hz |
| Fv2 ripple | R | 1 | - |
| Bandwidth | s_v | 20.6 | Hz |
| Phase margin | P_{mv} | 60 | Degree |
| Gain margin | G_{mv} | 8.2 | Db |

So, the open loop transfer function of outer force control is strongly affected by the human response. Referring to the Bode plot of Fig. 8 the human zero introduces an amplification which is very important for force control performance and stability. Asymptotic constant amplitude for $s > s_g$ does not depend on the human stiffness:

$$\left. \frac{F_u}{X_m} \right|_{s=s_g} \approx K_t \frac{M_u}{M_g + M_u}$$

For this reason, assuming that the mass of the human does not vary sensibly from subject to subject, the worst case for the stability corresponds to the condition of maximum human stiffness. Indeed, the higher the human stiffness, the higher the human zero frequency is and therefore the higher the phase lag. Nevertheless, force control performances increase if human stiffness increases: this is an intrinsic characteristic of the chosen control architecture. The haptic device can reach desired interaction force, by means of end-effector movement, as much as external environment offers resistance to end-effector movement. So, in order to maximize the force control performance in the worst case, a second-order Butterworth filter is inserted in the forward side of the controller. Centering the filter cut-off frequency in $s_{u',max}$ (i.e., for maximum value of K_u), the asymptotic Bode plot, again, becomes a constant line till s_g . This filter allows to attenuate the open loop magnitude for frequencies over $s_{u',max}$ and so to increase the force constant gain. Nevertheless, unavoidable variation of human stiffness modifies the Bode plot as shown in Fig. 12.

Stabilizing force control loop for $K_{u,max}$ will ensure that the control loop will be stable for all subjects with lower stiffness. In ideal conditions, force constant K_F , which allows a force bandwidth s_F equal to velocity bandwidth s_v , results in:

$$K_F = \frac{s_v}{K_{u,max}}$$

In general, this is only an upper limit value; in fact, the phase lag of the inner velocity loop imposes a reduction of the real force bandwidth.

Final force control parameters and performances are reported in Table 3 and Fig. 13 shows the Bode diagram of closed loop velocity controller.

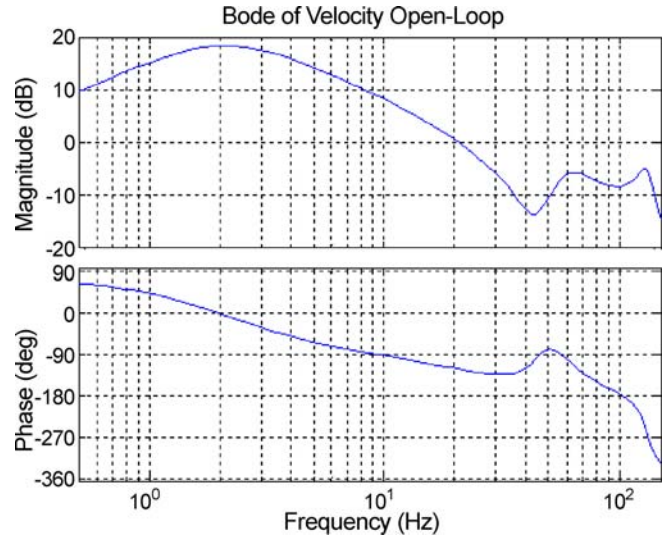
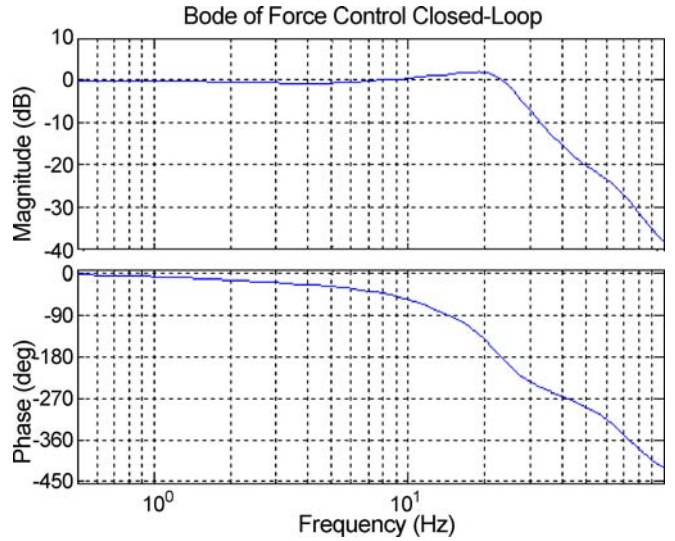

Fig. 11. Open loop Bode plot of velocity

Fig. 12. Bode plot in presence of human

Table 3. Force control parameters in presence of human

| Parameter | Sym. | Value | Unit |
|----------------------|----------|-------|--------|
| Force gain | K_f | 0.52 | m/sN |
| Ff cut-off frequency | F_f | 7.1 | Hz |
| Ff order | N_f | II | - |
| Bandwidth | s_f | 23.6 | Hz |
| Phase margin | P_{mf} | 54.4 | Degree |
| Gain margin | G_{mf} | 5.9 | Db |

Regarding the force control performances, it's important to note that in ideal static conditions (end-effector speed equal to zero), percentage force error is given

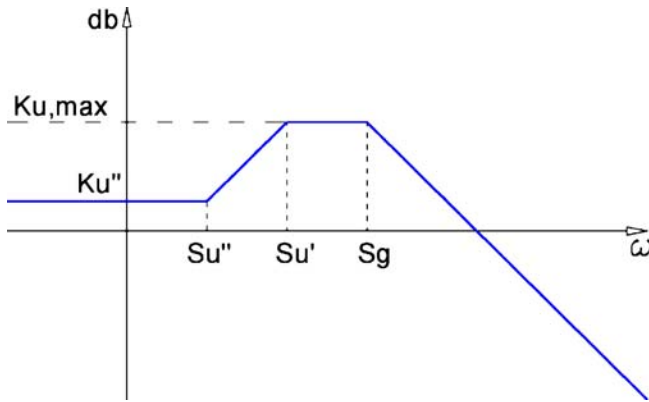


Fig. 13. Asymptotic Bode plot of transfer function due to presence of human

by:

$$\frac{F_{des} - F_u}{F_{des}} = \frac{1}{K_v K_f} = 1.96\%$$

during the movement at zero desired force, supposing the mechanical device is completely transparent, the disturbance force introduced by the controller is

$$F_{dist} = -\dot{X}_u \frac{K_v}{1 + K_v K_f} \approx -\dot{X}_u \frac{1}{K_f}$$

For example, a disturbance force of 0.2 N corresponds to an end-effector speed velocity of 0.1 m/s.

6 Field test

In order to experimentally evaluate the performance of the explicit force controller dimensioned according to the methodology described above, two sets of experiments have been carried out. In both sets, the subjects were asked to move their finger back and forth at an almost constant

velocity, resting for a while at the reversing of the motion direction.

The first test was carried out with a zero force control reference: the forces measured during the test are shown in Fig. 14a. In the second set the same test was then executed with a 1 N force control reference (Fig. 14b).

The tests show that the system is highly accurate in static conditions (as expected, error is less than 2%), while errors proportional to the end-effector velocity are introduced in dynamic conditions. This is an intrinsic characteristic of the selected basic architecture of the controller. In order to reduce the values of the resistant forces during the tracking at constant velocity the force gain K_F should be increased but this would lead to instability of the system.

7 Conclusion

In this paper we presented a novel haptic system and the design of its controller for an optimal combined haptic/tactile rendering in multi-sensory exploration of virtual textiles. The novel control design methodology is based on the identification of human and device parameters and its performances have been assessed both with theoretical analyses as well as with experimental validation.

An architecture to integrate this system in a multi-layer architecture that is suited for reproducing interaction with virtual clothes has been discussed and its implementation is available in our laboratory.

The overall architecture has proved to performing enough to support a wide range of feedback forces. Maximum accuracy has been assessed in both textile interaction condition: exploration and manipulation. In the first case, contact force is approximately 0, the force-feedback accuracy is below 1 gram in static condition while it holds within 10 grams in dynamic conditions; in the second case the force accuracy has proven to be within 5% of the overall applied force both in static and dynamic conditions.

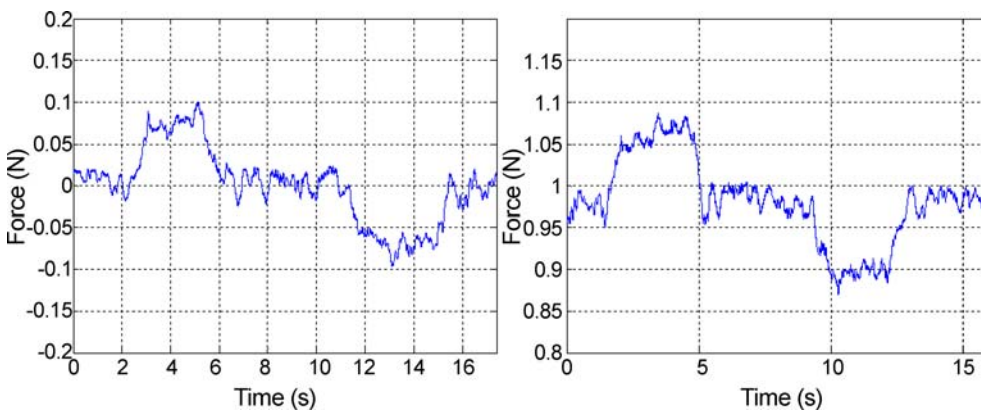
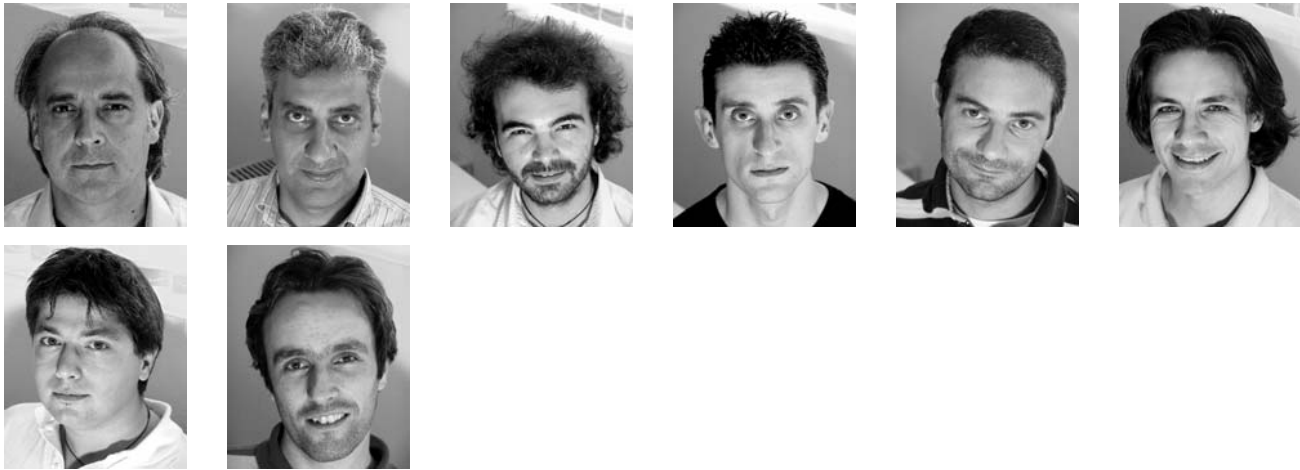


Fig. 14. Force measurements in field tests

References

- Adams, R.J., Hannaford, B.: Control law design for haptic interfaces to virtual reality. *IEEE Trans. Control Syst. Technol.* **10**(1), 3–13 (2002)
- Astley, O.R., Hayward, V.: Multirate haptic simulation achieved by coupling finite element meshes through Norton equivalents. In: *Proceedings of the 1998 IEEE International Conference on Robotics and Automation*, vol. 2, pp. 989–994, 16–20 May (1998)
- Avizzano, C.A., Marcheschi, S., Angerilli, M., Fontana, M., Bergamasco, M.: A Multi-Finger Haptic Interface for Visually Impaired People. In: *Proceedings of the 2003 IEEE International Workshop on Robot and Human Interactive Communication*, Millbrae, CA, 31 October–2 November (2003)
- Bridson, R., Marino, S., Fedkiw, R.: Simulation of clothing with folds and wrinkles. In: *Proceedings of ACM/Eurographics Symposium on Computer Animation*, pp. 28–36 (2003)
- De, S., Srinivasan, M.A.: Thin walled models for haptic and graphical rendering of soft tissues in surgical simulations. *Medicine Meets Virtual Reality. Stud. Health Technol. Inform.* **62**, 94–99 (1999)
- Eppinger, S., Seering, W.: Understanding bandwidth limitations in robot force control. In: *Proceedings of the 1987 IEEE International Conference on Robotics and Automation*, vol. 4, pp. 904–909, March (1987)
- Fagergren, A., Ekeberg, O., Forssberg, H.: Precision grip force dynamics: a system identification approach. *IEEE Trans. Biomed. Eng.* **47**(10), 1366–1375 (2000)
- Frank, A.O., Twombly, I.A., Barth, T.J., Smith, J.D.: Finite element methods for real-time haptic feedback of soft-tissue models in virtual reality simulators. In: *Proceedings of Virtual Reality 2001*, IEEE 13–17, pp. 257–263 (2001)
- Govindaraj, M., Garg, A., Raheja, A., Huang, G., Metaxas D.: Haptic Simulation of Fabric Hand. In: *Proceedings of Eurohaptics Conference* (2003)
- Hajian, A.Z., Howe, R.D.: Identification of the mechanical impedance at the human finger tip. In: Radcliffe C.J. (Ed.) *Proceedings of International Mechanical Engineering Congress*, American Society of Mechanical Engineers, Chicago, IL, November, DSC-vol. 55-1, pp. 319–327 (1994)
- Hauth, M., Etmuss, O.: A high performance solver for the animation of deformable objects using advanced numerical methods. In: Chalmers A., Rhyne T.-M. (Eds.) *Proceedings of Eurographics 2001*. *Comput. Graph. Forum* **20**(3), 319–328 (2001)
- Hui, C.L.: Neural Network Prediction of Human Psychological Perceptions of Fabric Hand. *Textile Res. J.* **May** (2004)
- Kawabata, S.: The Standardization and Analysis of Hand Evaluation, 2nd edn. The Hand Evaluation and Standardization Committee (HESC), The Textile Machinery Society of Japan, Osaka (1980)
- Salsedo, F., Fontana, M., Tarri, F., Ruffaldi, E., Bergamasco, M., Magnenat-Thalmann, N., Volino, P., Bonanni, U., Brady, A., Summers, I., Qu, J., Allerkamp, D., Böttcher, G., Wolter, F.E., Mäkinen, M., Meinander, H.: Architectural Design of the Haptex System. In: *Proceedings of the HAPTEX'05 Workshop on Haptic and Tactile Perception of Deformable Objects*, Hanover, pp. 1–7, December (2005)
- Ueberle, M., Buss, M.: Control of kinesthetic haptic interfaces. In: *Proceedings of IEEE/RSJ International Conference on Intelligent Robotics and Systems, Workshop on Touch and Haptics* (2004)
- Ueberle, M., Mock, N., Buss, M.: VISHARD10, a novel hyper-redundant haptic interface. In: *Proceedings of 12th International Symposium on Haptic Interfaces for Virtual Environment and Teleoperator Systems, HAPTICS '04.*, 27–28 March, pp. 58–65 (2004)
- Wen, K., Neacsulescu, D., Basic, G.: Development system for a haptic interface based on impedance/admittance control. In: *Proceedings of the 3rd IEEE International Workshop on Haptic, Audio and Visual Environments and Their Applications, HAVE 2004*, 2–3 October, pp. 147–151 (2004)
- Yoshikawa, T., Ichinoo, Y.: Impedance identification of human fingers using virtual task environment. In: *Proceedings of IEEE/RSJ International Conference on Intelligent Robots and Systems (IROS 2003)*, 27–31 October, vol. 4, pp. 3094–3099 (2003)



MASSIMO BERGAMASCO is a Full Professor of Applied Mechanics. He teaches the mechanics of robots and also virtual environments. His research activity deals with the study and development of haptic interfaces for the control of the interaction between humans and virtual environments. In this field he is interested in the kinematics aspects of the design of haptic mechanisms. He has been the scientific coordinator of several national projects and EU projects. Massimo Bergamasco is presently the Coordinator of the ENACTIVE Network of Excellence and the SKILLS Integrated Project. He has been author or coauthor of more than 200 papers in international scientific journals and conferences.

CARLO ALBERTO AVIZZANO is a Senior Researcher at Scuola Superiore Sant'Anna, and external Prof. of Mechatronics at University of Pisa. He graduated in Informatic Engineering with *summa cum laude* from the University of Pisa in 1995, and received the University Diploma in Engineering (1995) and Ph.D. in Robotics and Teleoperation in Virtual Environments (2000) from Scuola Superiore Sant'Anna.

Carlo Alberto Avizzano research interests relate the automation and digital control of robotic systems, and includes the design applied system in the fields of haptics control, teleoperation, simulators, mobile robotics, and advanced learning systems.

He has authored about 100 publications in international scientific journals and conferences.

ANTONIO FRISOLI is an Assistant Professor of Mechanical Engineering at Scuola Superiore Sant'Anna, where he is currently head of the Virtual Reality & Telerobotic Systems Division of Percro Laboratory.

He graduated in Mechanical Engineering with *summa cum laude* from the University of Pisa

in 1998, and received the University Diploma in Engineering and Ph.D. in Robotics and Teleoperation in Virtual Environments from Scuola Superiore Sant'Anna, respectively in 1998 and 2002.

His research interests are in the fields of haptic rendering and haptic interfaces design, robotics, automatic control, theoretical kinematics; in these fields he has authored more than 70 publications in international scientific journals and conferences.

FABIO SALSEDO since 1994 he has been responsible for the coordination of the research and development activities of the Mechanical Design Division at the PERCRO. Since 1995 he has played a major role in several national and international RTD projects.

At present he is the project manager of the national RTD project Body Extender and to the EU funded RTD project HAPTEX (HAPTic sensing of virtual TEXTiles).

His main interests are in the mechanical design of advanced haptic and human computer interfaces. He is coauthor of more than 10 international patents relating to haptic interfaces, mechanical motion tracking devices and robotic surgical tools.

EMANUELE RUFFALDI is currently a research fellow of the PERCRO Lab of Scuola Superiore S. Anna, Pisa, Italy. He obtained his Ph.D. in Perceptual Robotics in 2006 from Scuola Superiore S. Anna discussing a thesis on perceptually inspired haptic algorithms. He received a M.Sc. degree in Computer Engineering in 2002. His research interests are in the fields of virtual reality, information visualization, haptics, and physical modeling.

SIMONE MARCHESCHI was a Ph.D. student at Scuola Superiore Sant'Anna until 2004; he

collaborates as a control engineer with PERCRO Laboratory on the same research topics. He has acquired competencies in mechanical design during the academic courses and in the realization of a haptic device for the office automation. During the Ph.D. courses he carried out a research program focused on the analysis and design of mechanical systems for haptic interfaces and the synthesis of control systems for virtual environments.

He was involved in several EU projects, i.e., GRAB, CREATE, VIRTUAL, and PURE FORM.

He is coauthor of several publications for the most important international conferences in the field of robotics and automation.

MARCO FONTANA received his degree from the University of Pisa in 2003 with a diploma thesis on the design of a low-cost mechanical head tracker. Since then he has collaborated with PERCRO in several internal and EU projects. His research interests are in the field of mechanical design haptic interfaces and hand-held tools for surgical applications. Currently he is a Ph.D. candidate in Robotics for Virtual Environment and member of the research division of Perceptual Devices at PERCRO.

FEDERICO TARRI received his degree in Mechanical Engineering at University of Pisa in December 2004. He developed his thesis at PERCRO Laboratory; the title of his thesis was "Analysis and design of an innovative actuation system for a millirobotic end-effector to be used in minimally invasive surgery." He has continued his work at PERCRO Lab. and has started his Ph.D. in Robotics with Scuola Superiore Sant'Anna of Pisa in 2005. Now he is working on MISAT and HAPTEX (<http://haptex.miralab.unige.ch>) projects.